Energy measurement of relativistic electron beams by laser Compton scattering

Ian C. Hsu, Cha-Ching Chu, and Chuan-Ing Yu
Department of Nuclear Science, National Tsing Hua University and Synchrotron, Radiation Research Center, Hsinchu, 30043, Taiwan
(Received 4 June 1996)

Laser Compton scattering by relativistic electrons provides the energy information associated with electron beams in an accelerator. Determining the electron beam energy by this method depends primarily on the signal to noise (S/N) ratio associated with laser Compton scattering. In this study, we propose a method to enhance the S/N ratio by synchronous measurement with a high peak power pulsed CO_2 laser. In this method, the pulsed CO_2 laser provides the gate trigger signals, and the delay times of the triggers are optimized to obtain a maximum S/N ratio. In the storage ring of Taiwan Light Source, a γ ray with the highest energy of 3.021 MeV was backscattered after the 0.1172 eV CO_2 laser photons colliding with the relativistic electrons. The S/N ratio is about 42.5 with the electron beam current being 19 mA. Also, the measured electron beam energy is 1.3058 GeV with relative uncertainty 0.13%. [S1063-651X(96)02011-9]

PACS number(s): 29.27.Fh, 41.75.Ht, 13.60.Fz

I. INTRODUCTION

Compton scattering of photons by free electrons is a simple quantum-electrodynamics process that is experimentally accessible. Since Compton [1] presented a semiquantum-mechanical treatment of such an interaction in 1922, many theoretical calculations of the characteristics of Compton scattering have been developed.

In 1963, Milburn [2] and Arutyunian and Tumanian [3] accurately predicted the production of quasimonochromatic photon beams by utilizing laser backscattered photons from an energetic electron beam. After the experimental proofs by Kulikov *et al.* [4] in 1964, Bemporad, Milburn, and Tanaka [5] at Cambridge Electron Accelerator (CEA) in 1965, and Sinclair *et al.* [6] at Stanford Linear Accelerator Center (SLAC) in 1969, backward Compton scattering has become a highly promising alternative of producing useful yields of quasimonochromatic polarized photons.

In 1969 at SLAC, Ballam *et al.* [7] performed a physics measurement using laser backscattered photons as a beam. In this experiment, a 1.78 eV photon beam from a ruby laser collided with 20 GeV electrons from the SLAC linac to produce γ rays of variable energies up to 5 GeV; this was with a flux of around 500 s^{-1}. The first γ-ray beam for nuclear physics research [8] was developed at the 1.5 GeV ADONE storage ring at Frascati National Laboratories. Polarized γ rays of up to 80 MeV were produced with fluxes of around 5×10^4 s^{-1} after the 2.41 eV pulsed photon bunches from an argon ion laser collided head-on with the 1.5 GeV electron bunches. A higher γ-ray flux was achieved by the Laser Electron Gamma Source (LEGS) project [9] at Brookhaven Laboratory in 1983. The electron beam energy of LEGS was almost a factor of 2 orders higher than that of ADONE. In LEGS, the larger stored beam current and the smaller beam cross section in the straight section contributed to a photon flux larger than 2×10^7 s^{-1}.

Laser Compton scattering by relativistic electrons can produce an intense and directional quasimonochromatic photon beam. In practical terms, this energetic photon beam as a light source can be used to investigate the photonuclear reactions, calibrate the energies and the efficiencies of detectors, record the medical images, and measure the electron beam parameters such as the beam energies, the transversal beam dimensions, and the electron beam polarization.

Laser Compton scattering techniques by electron beam have prominent applications in many high-energy physics experiments. For instance, the Large Electron Positron (LEP) Collider beam energy measurement [10] by resonant spin depolarization at CERN in 1992 employed this technique in determining the electrons' spin polarization. The electron beam profile in the Next Linear Collider is in the order of several nanometers, and the technique of laser Compton scattering is supposed to be a practical method to measure the electron beams' transversal dimensions [11].

Two conventional approaches of measuring the electron beam energy are to measure the depolarization resonance and measure the magnetic field strength of the bending magnets. The depolarization resonance [10] method has the smallest relative energy uncertainty, e.g., 10^{-5}; however, this method involves the complexity of measuring the electron beam polarization. The relative energy uncertainty of measuring the magnetic field strength is around the order of 0.5%. In this study, we propose a method capable of providing an intermediate relative energy uncertainty with an easier measurement setup than that of the depolarization resonance method.

Here the electron beam energy is measured by using laser Compton scattering. The method we presented can be applied to any high-energy ($\gamma\gg1$) electron beam. The experiment is performed on the electron beam in the storage ring of Taiwan Light Source (TLS) of Synchrotron Radiation Research Center (SRRC), Taiwan. The techniques include aligning and focusing for far infrared, synchronously measuring the backscattered photons, and reducing background radiation from Bremsstrahlung.

To acquire a high γ-ray flux, a pulsed CO_2 laser with up to 2.67 MW peak power is employed. Owing to the fact that the background radiation from bremsstrahlung is extremely high (about 1200 s^{-1} at 20 mA electron beam current) and the time duration for γ rays to be produced is quite short (less than 60 ns per pulse), how to effectively subtract the background radiation is a relevant concern. In this study, we develop the method of synchronous measurement to resolve

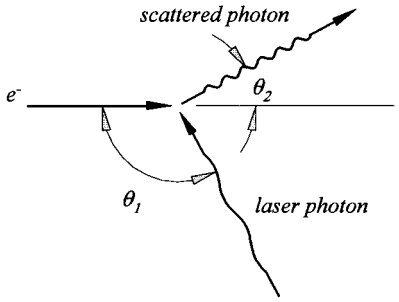

FIG. 1. Schematic diagram of laser Compton scattering.

the above problem. The method proposed herein increases the signal to noise ratio from 1.2 to 42.5. Also, to enhance the collision rate, we develop a simulation program to optimize the optics system. The relative energy measurement error of this experiment is 0.13%.

The techniques of laser Compton scattering developed in this study will contribute toward the development of tunable x-ray sources and that of a future free-electron laser (FEL) facility in the booster of TLS. The tunable wavelengths enable the tunable x-ray sources and the FEL to be highly effective tools in many applications such as medical image recording, nuclear physics research, and industry.

II. THEORY

Feenberg and Primakoff [12] proposed the kinematics formulas for Compton scattering on moving electrons in 1948. Figure 1 schematically illustrates the scattering process with angles greatly exaggerated. In this figure, the laser photon and the electron approach each other at some relative angle θ_1. After backscattering, the γ ray emerges at a small angle θ_2 relative to the electron's direction. The γ-ray energy is then given by

$$E_\gamma = \frac{E_L(1-\beta\cos\theta_1)}{(1-\beta\cos\theta_2)+E_L(1-\cos\chi)/E_e}, \tag{1}$$

where E_L is the incident laser photon energy, E_e is the incident electron energy, $\chi=\theta_2-\theta_1$, and $\beta=\nu/c$ with ν and c the velocities of the electron and light.

The above equation indicates that the γ rays with maximum energy $E_{\gamma,\max}$ travel at $\theta_2=0$ relative to the electron's direction in the case of a head-on collision. Since the final energy is uniquely determined by the angle θ_2 for a fixed θ_1, a collimator in the backward direction will narrow the photon spectrum to a confined region between $E_{\gamma,\max}$ and some low-energy cutoff $E_{\gamma,\text{cutoff}}$.

In 1928, Klein and Nishina derived the differential cross section associated with Compton scattering by free electrons. In the case of Compton scattering by moving charged particles, the formula can be expressed in the laboratory frame as [3]

$$\frac{d\sigma}{dE_\gamma}=\frac{\pi r_0^2}{2}\frac{m_0^2c^4}{E_LE_e^2}\left[\frac{m_0^4c^8}{4E_L^2E_e^2}\left(\frac{E_\gamma}{E_e-E_\gamma}\right)^2-\frac{m_0^2c^4}{E_LE_e}\frac{E_\gamma}{E_e-E_\gamma}+\frac{E_e-E_\gamma}{E_e}+\frac{E_e}{E_e-E_\gamma}\right], \tag{2}$$

where r_0 is the classical electron radius, m_0 is the rest mass of the electron, E_L is the incident laser photon energy, E_γ is the backscattered photon energy, and E_e is the electron beam energy.

The photon yield Y for each laser pulse scattered by a relativistic electron beam is given by [13]

$$Y=\frac{2N_eP\sigma d}{AcE_L}, \tag{3}$$

where N_e is the total number of electrons, P is the peak power of laser pulses, σ is the total interaction cross section, E_L is the incident laser photon energy, d is the interaction length, c is the velocity of light, and A is the smaller of the transverse photon beam size and the transverse electron beam size.

III. ESTIMATED MEASUREMENT ERRORS OF BACKSCATTERED PHOTON ENERGIES

The measurement errors of the backscattered photon energy depend primarily on energy distributions of the laser photons and the electron beams, electron beam divergence, electron beam size, system alignment, and the detector's resolution.

Discussion so far has considered the energies of laser photons and electrons to be uniform. In reality, however, the energy distributions for both the laser light and the electron beams are Gaussian.

The linewidth of the TEM_{00} mode laser beam is assumed here to be ΔE_L. The subsequent energy deviation for the backscattered photons is [13]

$$\frac{\Delta E_s}{E_s}\cong\frac{\Delta E_L}{E_L}. \tag{4}$$

For an energy deviation ΔE_e of the electron beams, the corresponding error of the backscattered photons is [13]

$$\frac{\Delta E_s}{E_s}\cong\frac{2\Delta E_e}{E_e}. \tag{5}$$

The fact that the electron beams have finite divergence and finite beam size does not affect the backscattered photons' highest energy. However, with the existence of the collimator, those factors decrease the photon yield at the highest photon energy. Equation (1) shows such a decrease, which is also confirmed by our spectrum simulation program [14].

The definition of the resolution at energy H_0 of the detector is [15]

$$R\equiv\frac{\mathcal{W}}{H_0},$$

where the full width at half maximum (FWHM) $\mathcal{W}$ is 2.35σ with σ the standard deviation of the spectrum of the single energy photons.

Since the errors from the energy distributions and the detector resolution are independent, the total errors of measuring the photon energy can be written as

$$\frac{\Delta E_s}{E_s}=\left[\left(\frac{\Delta E_L}{E_L}\right)^2+\left(\frac{2\Delta E_e}{E_e}\right)^2+\left(\frac{\mathcal{W}/2.35}{E_s}\right)^2\right]^{1/2}. \tag{6}$$

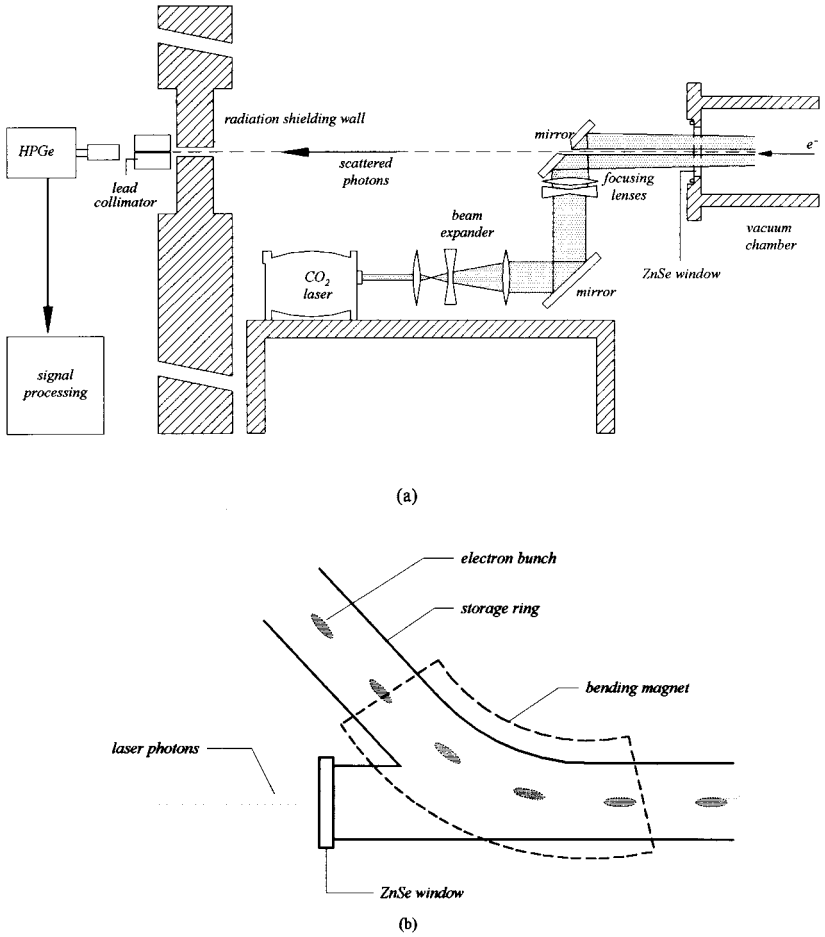

FIG. 2. (a) Schematic diagram of the overall system: part of the vacuum chamber of the storage ring, optical system, detecting system, and signal processing system; (b) top view of part of the vacuum chamber of the storage ring.

Using the error propagation method at the highest backscattered photon energy E_s, one can derive the electron beam energy measuring error ΔE_m as [13]

$$\frac{\Delta E_m}{E_e}=\frac{1}{2}\left[\left(\frac{\Delta E_s}{E_s}\right)^2+\left(\frac{\Delta E_L}{E_L}\right)^2\right]^{1/2}. \tag{7}$$

Suppose that the electron beam energy $E_e=1.3$ GeV, $\Delta E_e=0.86$ MeV, the FWHM at 3.021 MeV is 10 keV, and $\Delta E_L/E_L=0.001$, then the corresponding relative energy measuring error is about 0.24% for the backscattered photons and about 0.12% in determining the electron beam energy.

IV. EXPERIMENTAL DESIGN

A. Experimental setup

The experiment was performed at the fourth straight section of the storage ring (R4A1 section) of Taiwan Light Source. The entire system consisted of the optical system, detecting system, and signal processing instruments. The optical system was located inside the radiation shielding wall of the storage ring, while the detecting system and the signal processing instruments were located outside the shielding wall. Figure 2 presents the entire system's schematic diagram.

According to this figure, the laser photons pass through the optical system into the storage ring's straight section. After being scattered by relativistic electrons, the γ rays pass through the lead collimator and are then detected by the HPGe detector. Later, the signal processing instruments acquire the backscattered γ rays' spectrum.

1. Optical system

The optical system consists of a pulsed CO_2 laser, a beam expander, mirrors, and focusing lenses. The CO_2 laser provides incident photons and the mirrors alter the optical path for the laser photons so that it collides with the electrons in the storage ring's straight section. After scattering, the electrons are bent by the bending magnets toward the storage ring's next section, while the laser photons are scattered backwards. The upper mirror is hollowed out for the backscattered photons to pass through to the high purity Ge (HPGe) detector along the incident photons' path. The beam expander enlarges the laser beam so as to minimize the power loss due to the hole on the upper mirror. Moreover, the expanded laser beam is sequentially focused by the focusing lenses to increase the backscattered photon yield.

The material of the lenses is ZnSe and the mirrors are coated with infrared enhanced silver for 10.6 μm since these materials have a lower absorption coefficient for far infrared. The discharging effect having appeared in a strong focusing case would reduce the laser light's power and therefore should be avoided in designing the lens arrangement.

Considering the extremely low detecting efficiency of the HPGe detector at a high energy [16], e.g., the absolute full energy peak efficiency is around 1.5×10^{-5} at 10 MeV, an appropriate laser wavelength must be selected such that the detector's efficiency is acceptable at the backscattered pho-

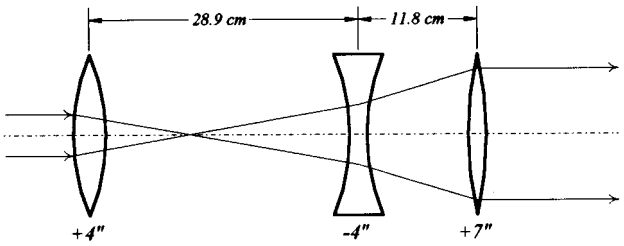

FIG. 3. Design of beam expander with a magnifying power of 5.

tons' maximum energy. According to Eq. (1), the backscattered photons' maximum energy was 48.42 MeV for a He-Ne laser ($\lambda=0.6328$ μm) and 29.49 MeV for a neodymium-doped yttrium aluminum garnet (Nd:YAG) laser ($\lambda=1.064$ μm) after Compton backscattering by 1.3 GeV electron beams. However, a CO_2 laser with a wavelength of 10.6 μm would produce the backscattered photons with a maximum energy around 3.021 MeV; this occurrence corresponds to an absolute full energy peak efficiency of around 2.0×10^{-4}. Therefore a CO_2 laser is selected in this experiment.

To increase the signal to noise ratio, a pulsed CO_2 laser was employed for its high peak power (up to 2.67 MW at repetition rate of 100 Hz). The pulse width was 30 ns and the energy per pulse was 87 mJ for the pulsed CO_2 laser.

The beam expander consisted of two convex lenses with focal lengths of $+4$ and $+7$ in. and a concave lens with a focal length of -4 in. In this experiment, the beam expander's magnifying power was 5 for a minimum power loss of the laser photons due to the hole on the upper mirror. The upper limit of the magnification power was set by the size of the ZnSe window. Figure 3 shows the beam expander's schematic diagram.

The focusing lenses were composed of a concave lens of focal length -5 in. and a convex lens of focal length $+7$ in. Our optics system simulation results [17] indicated that, for the maximum photon yield, the optimized focal length of the lens combination was 4.5 m.

2. Detecting system

The detecting system consisted of a lead collimator and an HPGe detector. The collimator was a hollowed cylinder with an inner diameter of 3 mm, an outer diameter of 100 mm, and was 100 mm long with a distance of 669.5 cm away from the end of the interaction region of the laser photons and the electron beams. After collimated, the backscattered γ rays were detected by the portable HPGe detector immediately behind the collimator.

3. Signal processing instruments

Using a pulsed CO_2 laser for its high peak power caused the scattered photons to be periodically produced with the same frequency as the CO_2 laser's repetition rate. The pulse length of CO_2 laser was 30 ns, and taking into account the maximum interaction length (10 m), the photons were produced within 60 ns for each laser pulse. However, the CO_2 laser's repetition rate was, at most, 200 Hz. This observation would suggest that the photons were produced within a time period less than 1.2×10^{-3}% of the total counting time. For instance, 3 h total counting time implies that the photons were produced for only about 0.1296 s. Besides, the continuous noise bremsstrahlung (which was produced due to the interaction between electron beams and the residual gases as well as ions) was markedly higher than the backscattered photons. Consequently, synchronously measuring the backscattered photons became an extremely important task.

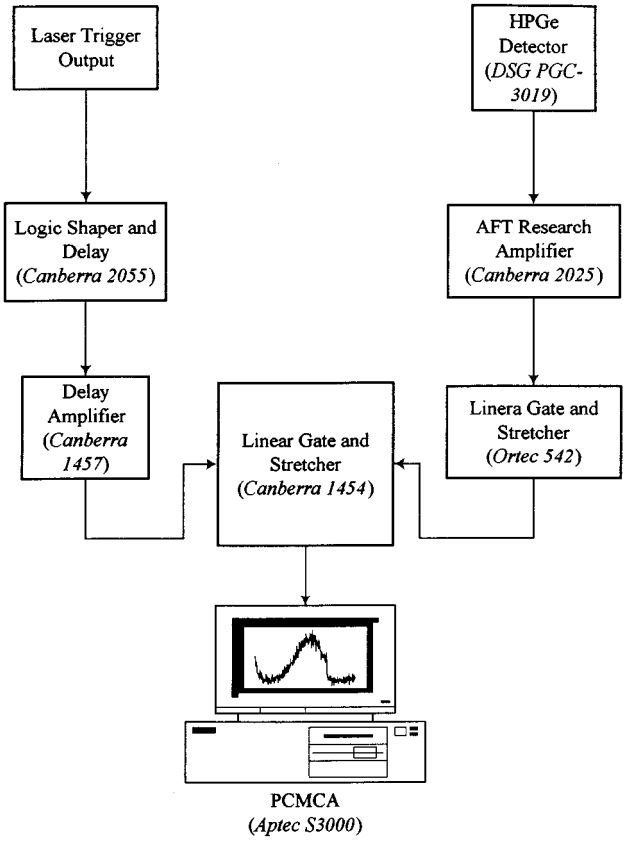

FIG. 4. Instruments associated with synchronous measurement.

The synchronous measurement used a gate to periodically allow the signals to pass from the detector to the counting system. Since the scattered photons were produced after the laser pulse reached the interaction region, the laser could provide a trigger signal for the gate to open. Figure 4 illustrates the experimental setup of synchronous measurement. As indicated in this figure, the laser trigger output provides the gate trigger signals which are first shaped and coarsely delayed by a logic shaper and delay. The trigger signals then pass through the delay amplifier for fine delay setting, i.e., to achieve a maximum counting rate. Meanwhile, the detector's signals are shaped by a linear gate and stretcher as well after passing through the preamplifier and the amplifier (automatic fine tuning research amplifier). Finally, the synchronous gate opens as triggered by the trigger signals and then allows the detector's signals to pass through to the PC multichannel analyzer
(PCMCA).

B. Photon yield equation modification

The upper mirror in Fig. 2 is hollowed with a hole having a diameter of 7 mm. The hole then causes a laser power loss for the sequential collisions. Since the geometric dimension of the laser beam is altered, Eq. (3) for the photon yield should be modified as [13,17]

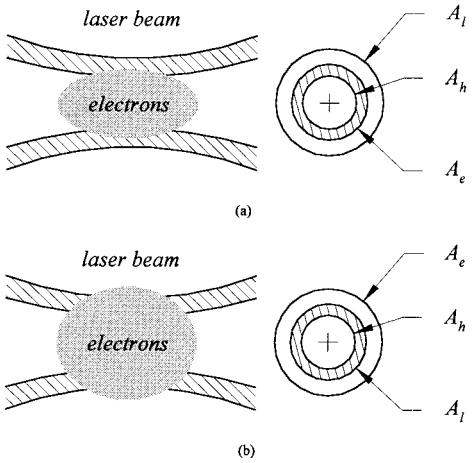

FIG. 5. Schematic diagram of the interaction between the laser beam and the electron bunch for (a) $A_l > A_e$ and (b) $A_l < A_e$, where A_l, A_e, and A_h are the cross sections of the laser beam, the electron beam, and the hole on the upper mirror, respectively.

$$Y = \frac{2P\sigma N_e}{cE_L} \int_{z_1}^{z_2} \left(\overline{A} - \frac{A_h}{A_e} \frac{I_h}{I_l} \right) \frac{dz}{\pi w^2}, \tag{8}$$

where $\overline{A}$ is A_l/A_e, A_l and A_e are the cross sections of the laser beam and the electron beam, respectively, A_h is the cross section of the hole of the laser beam after passing through the hollowed mirror, and

$$I_h = \int_0^{2\pi} \int_0^{w_{hm}} e^{-2r^2/w_{lm}^2} \frac{r dr d\theta}{\pi w_{hm}^2},$$

$$I_l = \int_0^{2\pi} \int_0^{w_{lm}} e^{-2r^2/w_{lm}^2} \frac{r dr d\theta}{\pi w_{lm}^2},$$

where w_{hm} is the radius of the hole on the upper mirror and w_{lm} is the spot size of the laser beam on the upper mirror. Figure 5 demonstrates the interaction between the hollowed laser beam and the electrons.

C. Energy calibration of HPGe detector

Considering that the highest energy of the backscattered photons was around 3000 keV, we chose ^{24}Na to be the standard source in energy calibration of the HPGe detector since the two characteristic energies of ^{24}Na were 1368.63 and 2754.03 keV. Those energies contributed to a sum-peak energy of 4122.66 keV which could be applied to the interpolation method in energy calibration. Figure 6 presents the ^{24}Na spectrum.

V. EXPERIMENTAL RESULTS AND DISCUSSIONS

A. Gate width limitation

Since the maximum gate width of the linear gate and stretcher (Canberra 1454) is 5 μs and the amplifier's shaping time is better for 4 μs (as suggested by the HPGe detector's test report), the gate would permit at most one signal to pass through to the PCMCA. This gate width limitation reduced the signal to noise (S/N) ratio and, subsequently, alleviated the spectrum's resolution.

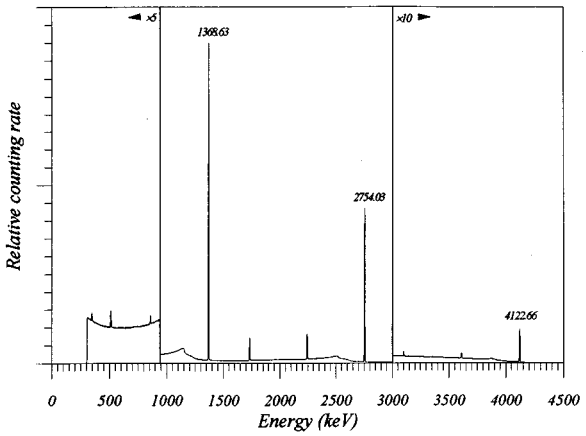

FIG. 6. ^{24}Na spectrum. A sum peak at 4122.66 keV is the accumulation of the two γ decay energies, 1368.63 and 2754.03 keV.

B. Optimization for gate delay setting

The gate delay setting was optimized through fine tuning the gate delay to obtain a maximum S/N ratio. Figure 7 illustrates the optimization process. This figure reveals that a maximum S/N ratio was obtained as the gate was delayed around 10.4 μs.

C. Energy cutoff by collimator

According to Eq. (1), the cutoff energy associated with the backscattered γ rays is determined by the collimator's inner diameter. Also, the collimator's half opening angle is 0.2241 mrad. Thus, for the case of $\theta_1 \cong \pi$, the theoretical cutoff energy is about 2.2987 MeV for 1.3 GeV electron beams.

D. Experimental results

Figures 8–11 display the spectra of the backscattered γ rays. Figure 8 presents the spectrum of the Compton scattering with a collimator having an inner diameter of 3 mm which corresponded to a half opening angle of 0.2241 mrad. The background radiation's counting rate without the laser Compton scattering effect was around 0.82 s^{-1}. After the laser photons collided with the electron beams, the counting rate rose to around 34.83 s^{-1}, i.e., the S/N ratio was approximately 42.5.

The following three figures demonstrate the importance of aligning the collimator, the collimator's size, and the synchronous measurement. Figure 9 stresses the importance of aligning the collimator. In this case, we used the same collimator size as was used to obtain the spectrum in Fig. 8. For an inadequately aligned system, the backscattered photons with the highest energy were either attenuated or stopped by the misaligned collimator which subsequently decreased the photon number and, ultimately, reduced the S/N ratio at that energy. The S/N ratio in this case was 9.0.

Figure 10 presents the spectrum of the Compton scattering with a collimator having an inner diameter of 10 mm

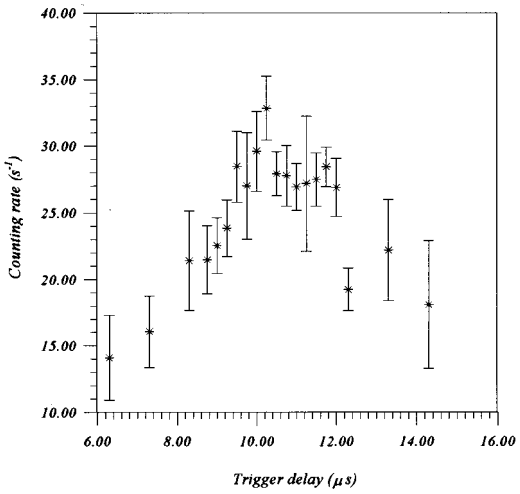

FIG. 7. Optimization of trigger delay for maximum S/N ratio. The optimum trigger delay in this case is 10.4 μs with S/N ratio $\cong$42.5.

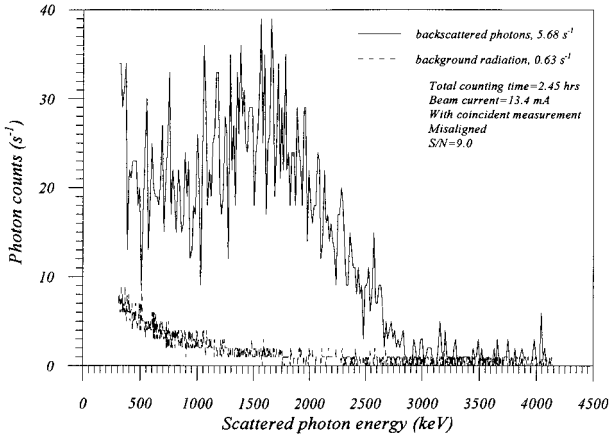

FIG. 9. γ-ray spectrum of Compton scattering with misaligned collimator of 3 mm diameter and under synchronous measurement (electron beam current, 13.4 mA; counting time, 2.45 h; and S/N ratio, 9.0).

which corresponded to a half opening angle of 0.818 mrad. The system was adequately aligned as was done to obtain the spectrum in Fig. 8. The electron beam current was 1.56 mA and, in this case, the S/N ratio was 5.0.

Figure 11 shows the spectrum obtained under the same conditions as in Fig. 8, but without synchronous measurement. In this case, the S/N ratio was only about 1.2. Comparing the two spectra reveals the significance of synchronous measurement. Apparently, the synchronous measurement could significantly enhance the S/N ratio.

E. Spectrum analysis and error estimation for energy measurement

Figure 12 denotes the method used to determine the highest photon energy associated with the laser Compton backscattering. This figure shows part of the spectrum in Fig. 8 for the energy above 2800 keV.

According to the theoretical spectrum of Compton scattering, the sharp edge at around 3 MeV indicates the highest backscattered photon energy, while after introducing the effects of the detecting efficiency, the detector's energy resolution, the energy distribution of laser photons, and the energy distributions of the electron beams to the spectrum, the edge is symmetrically distributed to both higher and lower energies. We can thus estimate the backscattered photon energy corresponding to the central energy of the electron beam at the middle point of the edge. Through some data processing, this photon energy can be derived as 3054 keV with a standard deviation of 2.6 keV. According to Eq. (1), the electron beams' central energy can be expressed as

$$\gamma=\frac{4E_L E_\gamma/m_0c^2+\sqrt{(4E_L E_\gamma/m_0c^2)^2+16E_L E_\gamma}}{8E_L}. \quad (9)$$

Offering E_γ=3054 keV, we obtain γ=2555.4 corresponding to the electron energy 1.3058 GeV, which is consistent with the results obtained from beam dynamics study [18] by Lee *et al.* of SRRC. In addition, our measured relative error for the electron beam energy is 0.13%.

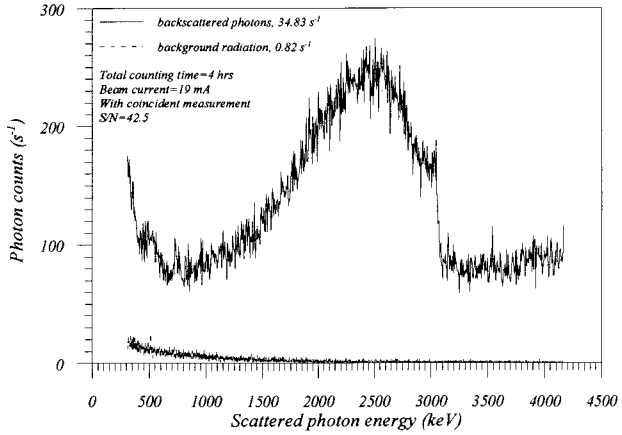

FIG. 8. γ-ray spectrum of Compton scattering with collimator of 3 mm diameter under synchronous measurement (electron beam current, 19 mA; counting time, 4 h; and S/N ratio, 42.5).

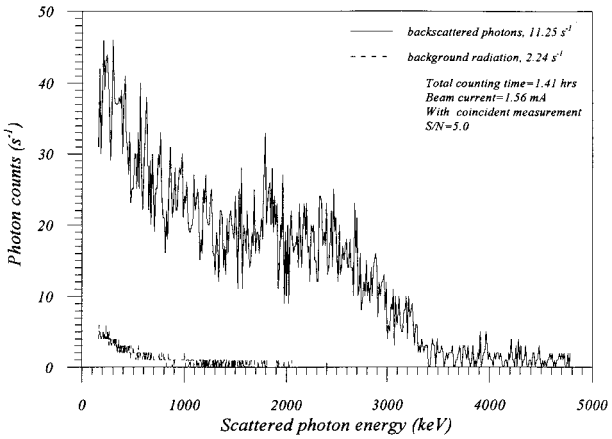

FIG. 10. γ-ray spectrum of Compton scattering with collimator of 10 mm diameter under synchronous measurement (electron beam current, 1.56 mA; counting time, 1.41 h; and S/N ratio, 5.0).

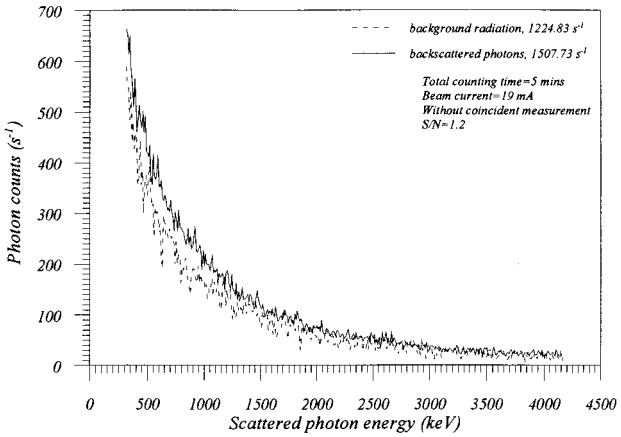

FIG. 11. γ-ray spectrum of Compton scattering with collimator of 3 mm diameter and without synchronous measurement (electron beam current, 19 mA; counting time, 5 min; and S/N ratio, 1.2).

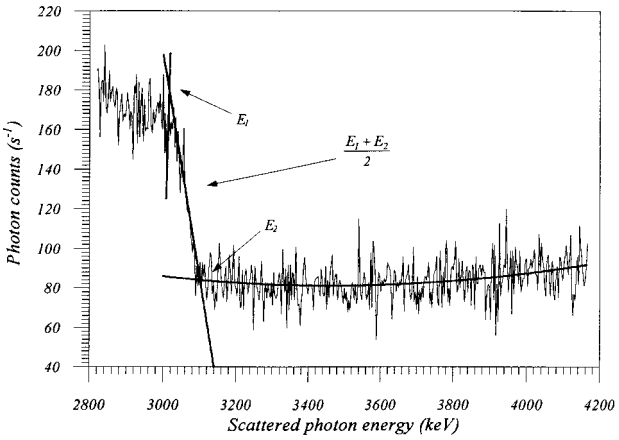

FIG. 12. Part of the spectrum in Fig. 8 for energy above 2800 keV. The method used to determine the highest backscattered photon energy.

VI. CONCLUSIONS

The synchronous measurement that contributes to a higher S/N ratio is the primary design feature of the laser Compton scattering experiment. This method employed the laser trigger outputs to trigger the gate. After the optimization process determined the optimum trigger delay to be 10.4 μs, a maximum S/N ratio was achieved at 42.5.

Since the backscattered photon energies were strongly angular dependent, precisely aligning the collimator and the optical system was deemed essential. The highest backscattered γ-ray energy could be estimated from the sharp edge of the spectrum as shown in Fig. 12. For our latest experiment, it was 3054 ± 2.6 keV. According to the results, we can infer that the electron beam energy was 1.3058 ± 0.0017 GeV. Further improvement includes using a larger gate width so that more backscattered photons can be counted and using a smaller collimator to sharpen the spectrum so that the photon energy corresponding to the electron central energy can be determined with higher precision.

Above techniques associated with laser Compton scattering can be used for establishing a tunable x-ray source and the FEL facility in the booster of TLS. The x-ray sources and the FEL facility will have tunable wavelengths for extensive applications in medicine, industry, and nuclear physics.

ACKNOWLEDGMENTS

We would like to thank the vacuum group, mechanical positioning group, instrumentation and control group, and radiation and safety group of SRRC, Taiwan, for their help in setting up the experimental apparatus. We also thank Professor Y. C. Liu, Professor S. G. Wu, Professor C. F. Wang, and Professor L. G. Yuan of National Tsing Hua University, Taiwan, for allowing us to use their instruments. Helpful discussions with Professor P. K. Tseng of National Taiwan University and Professor S. Y. Lee of Indiana University, Indiana, are appreciated. This study was supported by the National Science Council of the ROC and SRRC for financial support under Contract No. NSC83-0208-M-007-123.

[1] A. H. Compton, Bull. Natl. Res. Counc. (U.S.) **20**, 19 (1922); Phys. Rev. **21**, 483 (1923).
[2] R. H. Milburn, Phys. Rev. Lett. **10**, 75 (1963).
[3] F. R. Arutyunian and V. A. Tumanian, Phys. Lett. **4**, 176 (1963).
[4] O. F. Kulikov, Y. Y. Telnov, E. I. Filippov, and M. N. Yakimenko, Phys. Lett. **13**, 344 (1964).
[5] C. Bemporad, R. H. Milburn, and N. Tanaka, Phys. Rev. **138**, 1546 (1965).
[6] C. K. Sinclair, J. J. Murray, P. R. Klein, and M. Rabin, IEEE Trans. Nucl. Sci. **NS-16**, 1065 (1969).
[7] J. Ballam *et al.*, Phys. Rev. Lett. **23**, 498 (1969).
[8] G. Matone *et al.*, in *Photonuclear Reactions*, edited by S. Costa and C. Schaerf, Lecture Notes in Physics Vol. 62 (Springer, Berlin, 1977), p. 149; L. Federici *et al.*, Nuovo Cimento B **59**, 247 (1980).
[9] A. M. Sandorfi *et al.*, IEEE Trans. Nucl. Sci. **NS-30**, 3083 (1983).
[10] L. Arnaudon *et al.*, Phys. Lett. B **284**, 431 (1992).
[11] T. Shintake, Nucl. Instrum. Methods A **311**, 453 (1986); V. E. Balakin *et al.*, Phys. Rev. Lett. **74**, 2479 (1995).
[12] E. Feenberg and H. Primakoff, Phys. Rev. **73**, 459 (1948).
[13] Chen-Lien Cho, Master thesis, National Tsing Hua University, Hsinchu, Taiwan, 1993 (unpublished).
[14] Ian C. Hsu *et al.*, in *Proceedings of the 4th European Particle Accelerator Conference, London, UK*, edited by V. Suller and Ch. Petit-Jean-Genaz (World Scientific, Singapore, 1994), p. 1740.
[15] Glenn F. Knoll, *Radiation Detection and Measurement*, 2nd ed. (Wiley, New York, 1989), p. 115.
[16] Glenn F. Knoll, Ref. [15], p. 435.
[17] Ian C. Hsu *et al.*, in *Proceedings of the 1993 IEEE Particle Accelerator Conference, Washington, D.C.*, edited by S. Corneliussen (IEEE Service Center, Piscataway, 1993), p. 2151.
[18] J. C. Lee *et al.* (unpublished).